

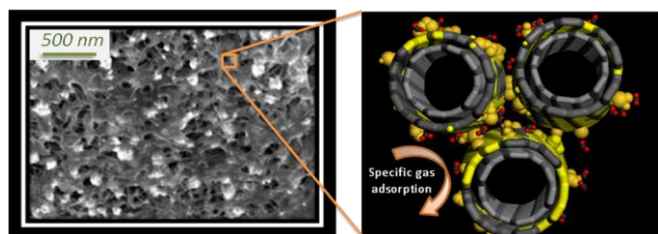
Activation of gold decorated carbon nanotube hybrids for targeted gas adsorption and enhanced catalytic oxidation

Ludovic Dumée^{aβ#}, Matthew R. Hill^{a#}, Mikel Duke^β, Leonora Velleman^δ, Kallista Sears^a, Jürg Schütz^a, Niall Finn^a, Stephen Gray^β

Abstract

Free standing assemblies of carbon nanotubes (CNTs), known as bucky-paper, (BP) have been functionalised through the *in-situ* plating of gold nanoparticles within the interstitial spaces in the BP. The nanoparticles are extremely small and well distributed at short plating times, so much so that the specific surface area of the BP is actually increased by the gold incorporation. These well distributed nanoparticles exhibit high enthalpy hydrogen storage and selective carbon dioxide adsorption over other gases, in particular methane. In concert with the conductive BP substrate, it has been demonstrated that these materials can also act as high turnover heterogeneous catalysts.

(Graphical abstract)



Keywords

gold decorated carbon nanotube; composite bucky-paper; specific gas storage; catalytic activity

Research highlights

- Design of super porous gold-CNT BP composites
- Controlled growth of NPs and even distribution across large BP samples through a novel approach
- Specific CO₂ adsorption over other gases and high H₂ enthalpy of adsorption
- Gold NPs enhanced the catalytic activity of the nanotubes

A. Introduction

Highly selective gas adsorbing materials have attracted wide interest as carbon capture and fuel cells, and thus stand as promising solutions to achieve sustainable development. While the major breakthroughs

achieved in the past decades followed routes targeting selective gas sieving via adsorption within nano-structured activated combinatorial materials,¹⁻¹⁰ processing large amounts of well organized materials such as metal nanoparticles (NPs)¹¹, Metal Organic Frameworks (MOFs) or zeolites remains a challenge.

Specific gas sensing and adsorption on metallic nano-particles (NPs) has been investigated due to their inherently high surface reactivity and thermo-mechanical stability over other materials. To date the highest H₂ storage capacity was reported in the case of metal hydrides¹² and noble metals (such as Pd, or Au). Although H₂ adsorption on gold surfaces was demonstrated to be weaker than on palladium (up to 900 times its volume of hydrogen¹³), gold catalytic activity was shown to be enhanced for gold NPs^{14, 15}. The presence of gold NPs on GaN nanowires¹⁶ was found to change the sensing capacity of the bare nanowires. For instance, the intensity/voltage characteristics of these hybrid ~ 5 nm NPs nanowires exposed to H₂, CH₄, CO₂ or CO was found to enhance by up to 4 fold when compared to that of air. The critical limitation of their development remains so far the processing and exposure of large surface areas of metallic NPs within highly porous matrices composed of a naturally high specific surface area material to optimize the surface to volume ratio. The adsorption¹⁷⁻²¹ and catalytic^{11, 15, 22-25} properties of gold are well documented following Haruta's work in the 90's²⁵ and sub 10 nm NPs were shown to be suitable adsorption sites due to their electronic d-bands becoming harder to saturate, creating semi-metallic structures more sensitive to selective gas adsorption^{14, 26}. The oxidation of CO by various sizes of gold NPs was found to be up to 100 times higher with sub 2 nm NPs when compared to sub 12 nm NPs, therefore highlighting the importance of exposed surface area on catalytic reactions²⁶.

Amongst the number of substrates available for NP growth, CNTs offer both a very high specific surface area and the advantage of being chemically and thermally^{27, 28} stable over a large range of temperatures. Specific modifications of the CNT outer graphene walls²⁹⁻³¹ have been repeatedly used as sites for targeted functionalisation and precursors for NPs decoration³²⁻³⁴. The enhanced electrochemical and catalytic properties of these metal decorated CNT composites^{33, 35-37} make them promising candidates for storage^{38, 39}, and sensing^{33, 34, 40-42} of gas^{43, 44} or chemicals⁴⁵⁻⁴⁷. Our approach in this work involves the growth of gold NPs by electroless deposition onto hydroxyl-functionalized CNTs. Free-standing assemblies of CNTs – called Bucky-papers (BPs), were used here as a growth support for their high specific surface area^{32, 42, 48} in order to expose large quantities of activated gold NPs within a confined volume.

Here we describe a route to plate BPs with gold NPs in confined volumes by electroless deposition⁴⁹ harnessing their highly porous (>90%⁵⁰) and mechanically stable structure. This is to the best of our knowledge, the first time that a route to grow gold NPs on CNTs within the pores of BPs has been proposed. Furthermore this route enables control of the composite porosity and NP size distribution. With such

control we then demonstrate their potential use as a gas storage media and catalyst.

B. Experimental section

1. Gold plating procedure

Self-supporting BPs were processed from chemical vapour deposition grown multi walled CNTs as described in a previous study⁵¹. In short, the functionalized CNTs were then suspended in propan-2-ol by 5 repeated cycles of freezing at -17 °C followed by bath sonication as per the method developed in⁵⁰. The CNT suspension was then filtered on top of a porous poly(ether sulphone) membrane to form a self-supporting BP. BPs were exposed for 10 min to a flow of UV induced ozone in order to form hydroxyl groups at the surface of outer CNT walls^{52, 53}. These groups are needed to both facilitate wetting of the CNTs by the plating solutions and as anchors for the initial plating reactions.

The procedure of electroless gold deposition within porous materials has been described by Martin et al.⁵⁴ and was previously used to fabricate pure gold nanotubes⁴⁸ in a three step protocol. During the first step, referred to as sensitization, the BPs were immersed in a tin solution of 20 0.026 M SnCl₂ and 0.07 M trifluoroacetic acid in a solvent of 50:50 methanol:water for 45 min followed by thorough rinsing in methanol for 5 min. Then in the second step, referred to as activation, the membrane was immersed in a solution of 0.029 M ammoniacal AgNO₃ for 30 min in order to plate the activated sites with silver, before being rinsed 25 sequentially in methanol and water to remove any unplated metals and remaining chemicals. In the third step, referred to as displacement deposition, the silver coated membrane was immersed in the gold plating solution consisting of 0.079 M Na₃Au(SO₃)₂, 0.127 M Na₂SO₃, 0.625 M formaldehyde and 0.025 M NaHCO₃. The temperature of this bath was 30 ~1–4 °C with pH = 8. Plating time was varied from 1 h up to 30 h, to control the amount of gold deposited, as well as the NP shape and the sample porosity. During the plating process depicted in⁴⁸ the gold cations were reduced on negatively charged sites on the CNTs and grew as particles of a few nanometres in dimension. All chemicals used in this 35 work were of analytical grade.

2. BP properties analysis

The gold content in the structure was determined by Thermo Gravimetric Analysis (TGA) (Perkin Elmer, TGA 7) with tests performed 40 at a rate of 10 °C/min and up to 900 °C. Porosity measurements were carried out on an Accu Pyc II 1340 Gas Displacement Pycnometer from Micromeritics at 19 Psi with Helium in a 1 cm³ chamber while BET specific surface area was obtained by N₂ adsorption at 77K on a Micromeritics Tristar 3000 after degassing the samples for at least 12 45 hours. Focused Ion Beam (FIB) milling was performed to produce Scanning Electron Micrographs (SEM) at 5 keV, 52 ° of tilt and 5 cm working distance. The Gallium (Ga) milling was performed with an initial

beam current of 7 nA followed by cleaning steps at 0.1 nA. Eventually, pore size distribution was determined by perm-porometry on a capillary 50 flow porometer from Porous Materials Inc. in wet-up/dry-up mode. Galwick and N₂ were respectively used as the wetting liquid and to pressurize the BP pores up to 500 psi.

3. Gas adsorption

The adsorption of N₂, CH₄ and CO₂ was performed at room 55 temperature while that of H₂ was obtained at both 77K (liquid N₂ temperature) and 87K (liquid Ar temperature) on selected samples that exhibited interesting adsorption behaviours using a Micromeritics ASAP 2420. The samples were degassed for 12 hours at 150 °C (Figure 6 – 60 supplementary materials).

4. Catalytic activity determination

BPs were exposed to pure analytical grade pentanal at 70 °C in oxygenated CDCl₃ for times of either 2 or 24 h. The composition of the 65 solution before and after being exposed to the catalytic influence of the BPs were analysed using Nuclear Magnetic Resonance (NMR) on a Bruker 400 MHz spectrometer.

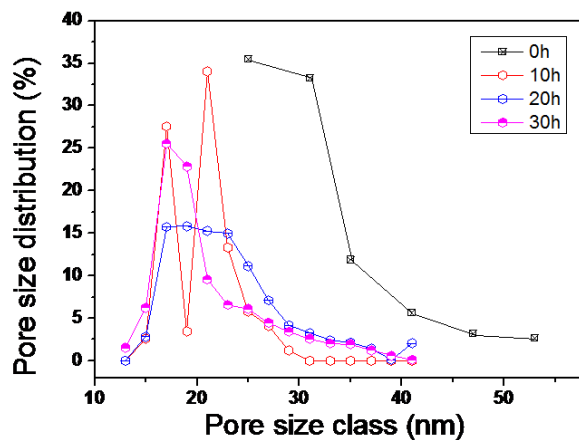
C. Results and Discussion

1. Materials properties

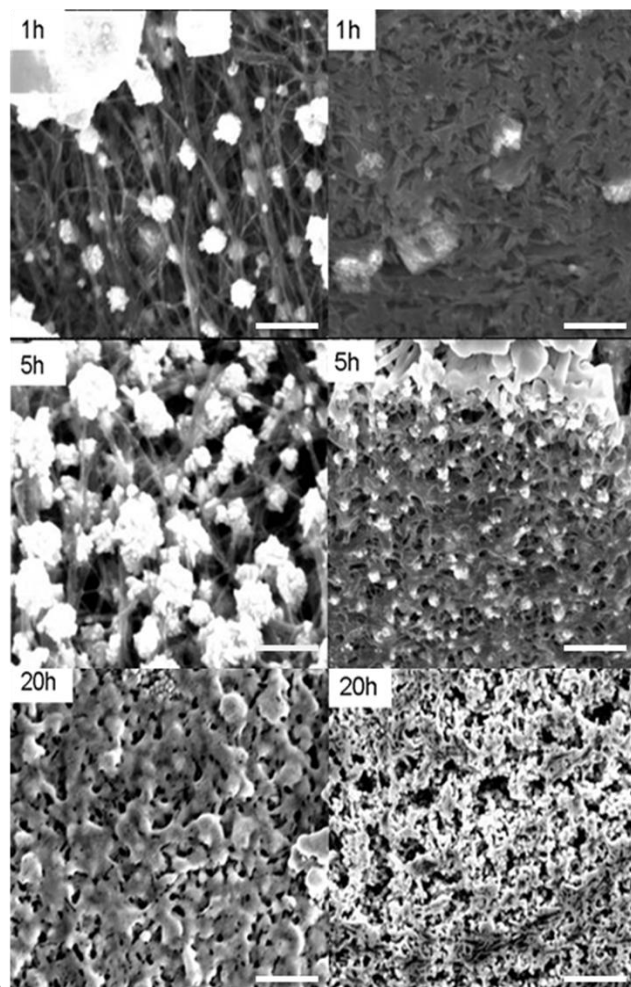
As shown in Table 1, the porosity and specific surface area of the BPs were clearly modified after gold deposition. Porosity decreased steadily from 90 % for the bare CNT BP down to 42% after 20 h of 75 plating. Furthermore, pore size distribution was also highly modified with increasing plating time. A clear shift in pore size was visible towards smaller pores (Figure 1) and tighter pore size distributions for increasing plating times. This is directly correlated to the amount of gold being deposited on the CNTs and to the formation of nano-clusters bridging the 80 CNTs. The inner structure of the BPs was revealed by Focused Ion Beam milling (FIB) of their surface and taking Scanning Electron Micrographs (SEM) and is presented in Figure 2. Gold NPs (10-50 nm) first formed on the CNT surface (Figure 2 – 1 h) before evolving into nano-clusters (1 h to 5 h) and then spreading between 5 h and 20 h towards an 85 interconnected network of continuous gold. After 20 h, the CNTs were uniformly coated and large nano-clusters emerged on the exposed gold surface.

TGA performed on the series of samples showed an initial diminished thermal stability which was attributed to the ozone treatment 90 inducing defects on the CNT walls. However, after 10 h of plating the stability, compared to a non treated sample, was recovered and improved. The samples were all stable up to 400 °C. The gold content calculated from the residual mass at 900 °C increased from 8 wt% after 1h of plating up to 90 wt% after 20h (Table 1).

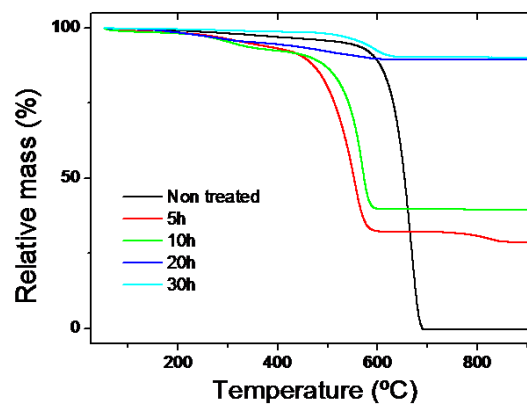
Furthermore, the material was found to be thermally stable with a mass loss of only 3-5 % up to 300 °C while severe degradation (95-97%) started occurring above 300 °C (Figure 3).



5 Figure 1 Pore size distribution determined by porometry at various plating times



10 Figure 2 SEMs of the surface (left column) and corresponding cross sections (right column) taken at different plating times; the cross sections were milled with a Gallium beam from a Focus Ion Beam (FIB) column in the SEM; scale bars correspond to 500 nm on all the SEMs



15 Figure 3 TGA analysis results with plating time as main parameter

2. Gas adsorption

20 Gas adsorption was employed to investigate the distribution of Au NPs as a function of plating time. Nitrogen adsorption (Table 1) revealed

that the specific surface area increases with plating times up to five hours, then subsequently decreases as plating continues. This indicates that the Au is initially deposited in nanoparticulate form, itself contributing to the surface area. Longer plating times increased the size of these particles, filling the voids and lowering the available surface area.

Successful exposure of the Au NPs on the BP surface was confirmed by measuring the enthalpy of adsorption towards hydrogen. Carbonaceous surfaces will typically adsorb hydrogen at around 4-5 kJ/mol⁵⁵ whereas metallated surfaces will form a stronger attraction to hydrogen, often between 5 to 50 kJ/mol depending on the metal alloy, surface roughness and crystallite morphology being tested⁵⁶⁻⁵⁸. Although the adsorption of extended gold surfaces has been demonstrated to be lower than that of other metals such as palladium or platinum⁵⁹, recent work also demonstrated that small gold clusters lead to enhanced adsorption of hydrogen^{60,61}. This is demonstrated in Figure 2 and Figure 4, where the average NP size was found to be around 52 and 300 nm (Table 1) for the 1 and 5h plated samples respectively. The plating time is therefore clearly controlling NP morphologies and sizes, thus influencing the overall adsorption process. The largest hydrogen physisorption is found to occur for the 5h plated sample giving a binding enthalpy, as high as 9.8 kJ/mol. The clustering of the gold NPs is found, after 5h of plating to lead to a semi-continuous network covering the surface of the CNTs and starting to fill the pores. It is therefore likely that shorter plating times would lead to smaller NP size distributions that could possibly even possess higher hydrogen adsorption capacity.

Exposed Au NPs also deliver selective gas adsorption, as shown in Figure 5. In particular, CO₂/CH₄ adsorption selectivity is as high as 11 at 900 mmHg. This is an important gas pair for industrial separations which could also lead to breakthrough towards more efficient and sensitive gas sensing materials.

Table 1 Properties of the Gold- CNT hybrid composites – the particle size was estimate from the SEM images in Figure 2

Samples	Gold content	Porosity	Specific surface area	NP size range
Plating time (h)	wt%	%	m ² /g	nm
0	0	90	197	N/A
1	8	85	310	10-50
5	28	76	229	50-300
10	89	63	88	N/A
20	90	42	37	N/A

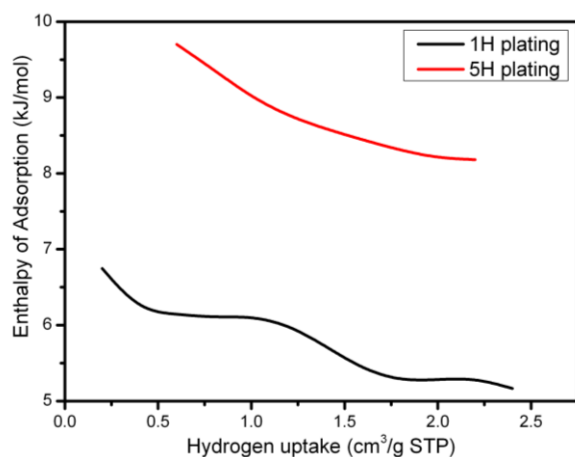


Figure 4 : The 5h Au plated BP sample (top curve) showed higher enthalpy of adsorption for H₂ than the 1h one (bottom curve)

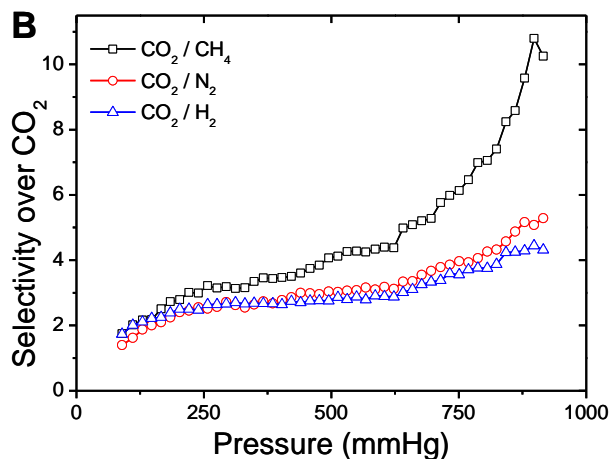
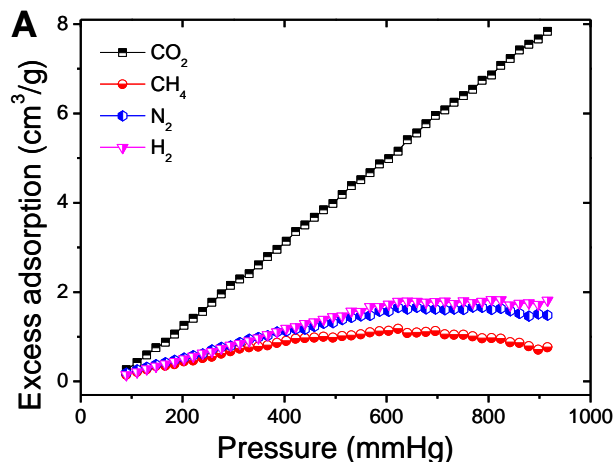


Figure 5 Gas excess adsorption (A) and relative selectivity for CO₂ (B) over the other gases for the 5 h plated sample at room temperature

3. Catalytic activity – pentanal decomposition

Gold is well known to play a part in catalytic oxidations.^{11, 15, 22-25}

Cost and recovery of the gold dictate that highly exposed surfaces that lower the amount of catalyst needed, or increase the reaction rates are desirable. A heterogeneous catalyst where the active material is affixed to a support is also desirable as it avoids complicated recovery processes. To demonstrate the effects of the well-dispersed gold upon the conductive carbon substrate, oxidation of pentanal to pentanoic acid was explored (Table 2). Oxygenated solutions of pentanal were exposed to functionalised and non-functionalised BP (normalised to carbon content) at 70 °C for 2 and 24 hours. Table 2 shows that the oxidation is significantly enhanced by the gold functionalised BP, whilst non-functionalised samples showed no significant change from the control sample.

Table 2 Catalytic decomposition of pentanal (%), when exposed to non-plated or gold plated CNTs for either 2 or 24 hours at 70°C

	Pentanal after 2h	Pentanal after 24h
	%	%
Control (no CNTs)	84.0	67.9
Non plated BP	91.1	70.2
1h Au plated BPs	64.3	36.7
10h Au plated BPs	36.5	12.2

D. Conclusions

A novel route to well-distributed gold NPss on a BP substrate has been shown for the first time. The well-distributed gold NPs were observed after only at short plating time, and lead to increased the surface area. High enthalpy hydrogen adsorption demonstrated well-exposed gold surfaces, which showed selective gas adsorption, useful in particular for CO₂/CH₄ separations. The combination with the conductive BP substrate proved to be effective for developing a high turnover rate heterogeneous catalyst. These materials offer new applications in separations and chemical conversions.

Notes and references

^a CSIRO Materials Science and Engineering, Clayton, Victoria, 3168, Australia

^β Institute for Sustainability and Innovation at Victoria University, Werribee, Victoria, 3030, Australia

^δ School of Chemical and Physical Sciences, Flinders University, Bedford Park, Adelaide, South Australia, 5042, Australia

1. H. Bux, C. Chmelik, J. M. van Baten, R. Krishna and J. Caro, *Advanced Materials*, **22**, 4741-4743.
2. S. T. Meek, J. A. Greathouse and M. D. Allendorf, *Adv. Mater. (Weinheim, Ger.)*, 2011, **23**, 249-267.
3. E. Poirier and A. Dailly, *Nanotechnology*, 2009, **20**, 204006.

4. C. Zlotea, R. Campesi, F. Cuevas, E. Leroy, P. Dibandjo, C. Volkringer, T. Loiseau, G. Férey and M. Latroche, *Journal of the American Chemical Society*, **132**, 2991-2997.
5. J. Ahn, W.-J. Chung, I. Pinnau and M. D. Guiver, *Journal of Membrane Science*, 2008, **314**, 123-133.
6. E. R. Hensema, *Advanced Materials*, 1994, **6**, 269-279.
7. K. Sumida, M. R. Hill, S. Horike, A. Dailly and J. R. Long, *Journal of the American Chemical Society*, 2009, **131**, 15120-15121.
8. M. C. Duke, J. C. D. da Costa, D. D. Do, P. G. Gray and G. Q. Lu, *Advanced Functional Materials*, 2006, **16**, 1215-1220.
9. M. C. Duke, J. C. Diniz da Costa, G. Q. Lu, M. Petch and P. Gray, *Journal of Membrane Science*, 2004, **241**, 325-333.
10. A. Tavorolo and E. Drioli, *Advanced Materials*, 1999, **11**, 975-996.
11. H. Sakurai, S. Tsubota and M. Haruta, *Applied Catalysis A: General*, 1993, **102**, 125-136.
12. W. P. Kalisvaart, C. T. Harrower, J. Haagsma, B. Zahiri, E. J. Lubber, C. Ophus, E. Poirier, H. Fritzsche and D. Mitlin, *International Journal of Hydrogen Energy*, 2010, **35**, 2091-2103.
13. W. Grochala and P. P. Edwards, *ChemInform*, 2004, **35**, no-no.
14. G. Bond, *Gold Bulletin*, 2010, **43**, 88-93.
15. H. Sakurai and M. Haruta, *Applied Catalysis A: General*, 1995, **127**, 93-105.
16. C. A. Berven, V. Dobrokhotov, D. N. McIlroy, S. Chava, R. Abdelrahman, A. Heieren, J. Dick and W. Barredo, *IEEE Sens. J.*, 2008, **8**, 930-935.
17. L. Stobinski and R. Dus, *Surface Science*, 1992, **269-270**, 383-388.
18. L. Stobinski, R. Nowakowski and R. Dus, *Vacuum*, 1997, **48**, 203-207.
19. V. M. Browne, A. F. Carley, R. G. Copperthwaite, P. R. Davies, E. M. Moser and M. W. Roberts, *Applied Surface Science*, 1991, **47**, 375-379.
20. N. Lopez, T. V. W. Janssens, B. S. Clausen, Y. Xu, M. Mavrikakis, T. Bligaard and J. K. Nørskov, *Journal of Catalysis*, 2004, **223**, 232-235.
21. S. Tibus, J. Klier and P. Leiderer, *Journal of Low Temperature Physics*, 2006, **142**, 83-89.
22. S. Wang, Y. Zhao, J. Huang, Y. Wang, S. Wu, S. Zhang and W. Huang, *Solid-State Electronics*, **50**, 1728-1731.
23. G. Musie, M. Wei, B. Subramaniam and D. H. Busch, *Coordination Chemistry Reviews*, 2001, **219-221**, 789-820.
24. K.-C. Wu, Y.-L. Tung, Y.-L. Chen and Y.-W. Chen, *Applied Catalysis B: Environmental*, 2004, **53**, 111-116.
25. M. Haruta, *Catalysis Today*, 1997, **36**, 153-166.
26. S. H. Overbury, V. Schwartz, D. R. Mullins, W. Yan and S. Dai, *Journal of Catalysis*, 2006, **241**, 56-65.
27. A. E. Aliev, C. Guthy, M. Zhang, S. Fang, A. A. Zakhidov, J. E. Fischer and R. H. Baughman, *Carbon*, 2007, **45**, 2880-2888.
28. J. Che, T. Cagin and W. A. G. III, *Nanotechnology*, 2000, **11**, 65-69.

29. T. Lin, V. Bajapi, T. Ji and L. Dai, *Aust. J. Chem.*, 2003, **56**, 635-651.
30. M. Majumder, N. Chopra and B. J. Hinds, *J. Am. Chem. Soc.*, 2005, **127**, 9062-9070.
- 5 31. J. Zhao, D. W. Schaefer, D. Shi, J. Lian, J. Brown, G. Beaucage, L. Wang and R. C. Ewing, *The Journal of Physical Chemistry B*, 2005, **109**, 23351-23357.
32. C.-Y. Chen, K.-Y. Lin, W.-T. Tsai, J.-K. Chang and C.-M. Tseng, *International Journal of Hydrogen Energy*, **35**, 5490-5497.
- 10 33. K.-Y. Lin, W.-T. Tsai and T.-J. Yang, *Journal of Power Sources*, **In Press, Corrected Proof**.
34. Y. Yun, Z. Dong, V. N. Shanov, A. Doepke, W. R. Heineman, H. B. Halsall, A. Bhattacharya, D. K. Y. Wong and M. J. Schulz, *Sensors and Actuators B: Chemical*, 2008, **133**, 208-212.
- 15 35. X. Chen, Y. Zhang, X. P. Gao, G. L. Pan, X. Y. Jiang, J. Q. Qu, F. Wu, J. Yan and D. Y. Song, *International Journal of Hydrogen Energy*, 2004, **29**, 743-748.
- 20 36. F. Tan, X. Fan, G. Zhang and F. Zhang, *Materials Letters*, 2007, **61**, 1805-1808.
37. J. John, E. Gravel, A. Hagege, H. Y. Li, T. Gacoin and E. Doris, *Angew. Chem.-Int. Edit.*, 2011, **50**, 7533-7536.
38. J. J. Zhao, A. Buldum, J. Han and J. P. Lu, *Nanotechnology*, 2002, **13**, 195-200.
- 25 39. S. M. Cooper, H. F. Chuang, M. Cinke, B. A. Cruden and M. Meyyappan, *Nano Letters*, 2003, **3**, 189-192.
40. D. R. Kauffman, Y. Tang, P. D. Kichambare, J. F. Jackovitz and A. Star, *Energy & Fuels*, **24**, 1877-1881.
- 30 41. M. Kaempgen, M. Lebert, N. Nicoloso and S. Roth, *Applied Physics Letters*, 2008, **92**, 3.
42. D. Yuan and Y. Liu, *Rare Metals*, 2006, **25**, 237-240.
43. H. Cong, J. Zhang, M. Radosz and Y. Shen, *Journal of Membrane Science*, 2007, **294**, 178-185.
- 35 44. R. Smajda, A. Kukovec, Z. Konya and I. Kiricsi, *Carbon*, 2007, **45**, 1176-1184.
45. N. A. Kashedikar and J. Maier, WILEY-VCH Verlag, 2009, pp. 2664-2680.
46. C. Liu, F. Li, L.-P. Ma and H.-M. Cheng, WILEY-VCH Verlag, pp. E28-E62.
- 40 47. S. H. Ng, J. Wang, Z. P. Guo, J. Chen, G. X. Wang and H. K. Liu, *Electrochimica Acta*, 2005, **51**, 23-28.
48. L. Velleman, J. G. Shapter and D. Losic, *Journal of Membrane Science*, 2009, **328**, 121-126.
- 45 49. L. Dumeé, L. Velleman, K. Sears, M. Hill, J. Schutz, N. Finn, M. Duke and S. Gray, *Membranes*, 2010, **1**, 25-36.
50. L. F. Dumée, K. Sears, J. Schütz, N. Finn, C. Huynh, S. Hawkins, M. Duke and S. Gray, *Journal of Membrane Science*, 2010, **351**, 36-43.
- 50 51. S. C. Hawkins, J. M. Poole and C. P. Huynh, *The Journal of Physical Chemistry C*, 2009, **113**, 12976-12982.
52. S. Agrawal, M. S. Raghuvver, H. Li and G. Ramanath, *Applied Physics Letters*, 2007, **90**, 193104-193104-193103.
53. M.-L. Sham and J.-K. Kim, *Carbon*, 2006, **44**, 768-777.
- 55 54. V. P. Menon, and Martin, C.R., *Anal. Chem.*, 1995, **67**, 1920-1928.
55. T. Ben, H. Ren, S. Ma, D. Cao, J. Lan, X. Jing, W. Wang, J. Xu, F. Deng, J. M. Simmons, S. Qiu and G. Zhu, *Angewandte Chemie International Edition*, 2009, **48**, 9457-9460.
56. C. Kartusch and J. A. van Bokhoven, *Gold Bull.*, 2009, **42**.
57. E. Bus and J. A. van Bokhoven, *Physical Chemistry Chemical Physics*, 2007, **9**, 2894-2902.
58. S. J. Holden and D. R. Rossington, *The Journal of Physical Chemistry*, 1964, **68**, 1061-1067.
- 65 59. S. A. C. Carabineiro and B. E. Nieuwenhuys, *Gold Bull.*, 2009, **42**.
60. L. Barrio, P. Liu, J. A. Rodriguez, J. M. Campos-Martin and J. L. G. Fierro, *The Journal of Chemical Physics*, 2006, **125**, 164715.
- 70 61. N. S. Phala, G. Klatt and E. v. Steen, *Chem. Phys. Lett.*, 2004, **395**, 33-37.

Supplementary information

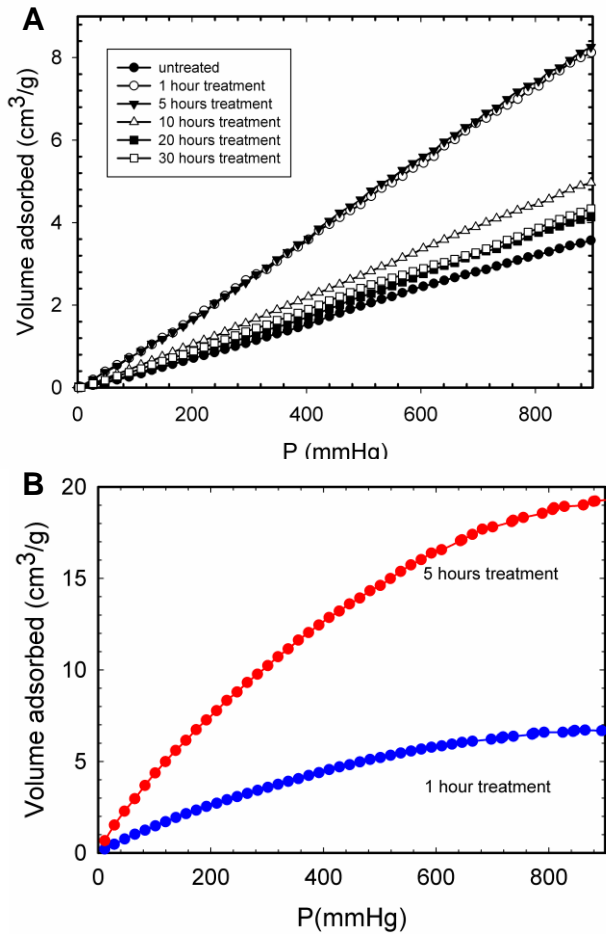


Figure 6 Evidence of CO₂ and H₂ adsorption on the different samples; A: CO₂ adsorption (volume - STP) measured at 293K on the series of samples; and B: H₂ volume adsorbed at 77 K for the 1 h and 5 h plated samples